DOI: 10.1534/genetics.106.060087

Mos1 Mutagenesis Reveals a Diversity of Mechanisms Affecting Response of *Caenorhabditis elegans* to the Bacterial Pathogen *Microbacterium nematophilum*

Karen Yook and Jonathan Hodgkin[1]

Genetics Unit, Department of Biochemistry, University of Oxford, Oxford OX1 3QU, United Kingdom

Manuscript received April 27, 2006
Accepted for publication November 15, 2006

ABSTRACT

A specific host–pathogen interaction exists between *Caenorhabditis elegans* and the gram-positive bacterium *Microbacterium nematophilum*. This bacterium is able to colonize the rectum of susceptible worms and induces a defensive tail-swelling response in the host. Previous mutant screens have identified multiple loci that affect this interaction. Some of these loci correspond to known genes, but many *bus* genes [those with a bacterially unswollen (Bus) mutant phenotype] have yet to be cloned. We employed *Mos1* transposon mutagenesis as a means of more rapidly cloning *bus* genes and identifying new mutants with altered pathogen response. This approach revealed new infection-related roles for two well-characterized and much-studied genes, *egl-8* and *tax-4*. It also allowed the cloning of a known *bus* gene, *bus-17*, which encodes a predicted galactosyltransferase, and of a new *bus* gene, *bus-19*, which encodes a novel, albeit ancient, protein. The results illustrate advantages and disadvantages of *Mos1* transposon mutagenesis in this system.

ALL animals and plants coexist with potentially lethal pathogens. Whether or not a pathogen infects a particular host, and whether an infection proves lethal, depends on the response of both the pathogen and host to these encounters. Most multicellular organisms rely on only two lines of defense against pathogens: a mechanical defense provided by the epidermis and an innate immune defense provided by germ-line-encoded pathogen recognition and antimicrobial factors and responses. Pathogen success relies on being able to exploit or evade these defenses. For example, carbohydrates on host surfaces are often targets for binding by pathogens (for examples see Johnson 1999). As the outer surfaces of nematodes such as *Caenorhabditis elegans* are composed mainly of sugar-modified proteins and lipids (for review see Blaxter and Bird 1997), it is not surprising to find that the surface of the worm is a site of adherence for pathogens (Jannson 1994; Mendoza de Gives *et al.* 1999; Hodgkin *et al.* 2000; Joshua *et al.* 2003; Hoflich *et al.* 2004).

Many studies have shown that *C. elegans* mounts conserved innate immune responses against invading pathogens. Specifically, evolutionarily distant organisms, such as plants, mammals, and nematodes, employ a p38 MAP kinase cascade or a TGFb pathway in defense against bacterial and fungal pathogens (for reviews see Millet and Ewbank 2004; Schulenburg *et al.* 2004; Gravato-Nobre and Hodgkin 2005; Sifri *et al.* 2005). Further, a nematode DAF-2 insulin-like receptor/IGF signaling pathway contributes to protection against pathogens (Garsin *et al.* 2003). This pathway is also implicated in environmental stress response pathways and longevity in *C. elegans* as well as other organisms (Kenyon *et al.* 1993; Tatar *et al.* 2003; Baba *et al.* 2005; Gami and Wolkow 2006). These studies have identified conserved host factors used against virulent pathogens with a generalized host range. However, host factors that have coevolved in response to pathogens with a narrow host range may have been missed.

When *C. elegans* is exposed to *Microbacterium nematophilum* it becomes sick and develops a swollen tail region, referred to as the deformed anal region (Dar) phenotype. Previous work has shown that this swelling response is mediated through the ERK/MAPK pathway (Nicholas and Hodgkin 2004). Worms with mutations in this pathway fail to swell after exposure to *M. nematophilum*; instead, these mutants experience severe constipation and greatly increased rate of larval arrest, adult sterility, or death. This implicates the ERK/MAPK pathway as a defensive signaling mechanism in the context of this infection.

Previous forward genetic screens have identified many loci that are involved in this host–pathogen interaction. From ethyl methanesulfonate (EMS) and *mut-7* transposon screens, >20 loci were found to affect tail swelling in the presence of *M. nematophilum*, which is a conspicuous and easily scored phenotype (Gravato-Nobre *et al.* 2005). Some of these loci correspond to known genes, but most have not been previously defined and were termed *bus* for *b*acterially *u*n*s*wollen—that is,

[1]*Corresponding author:* Genetics Unit, Department of Biochemistry, University of Oxford, S. Parks Rd., Oxford OX1 3QU, United Kingdom. E-mail: jonathan.hodgkin@bioch.ox.ac.uk

worms exposed to the pathogen fail to swell, either because infection fails or because the swelling response is defective. These screens have not reached saturation. Specifically, there are many *mut-7*-induced loci for which an EMS allele was not obtained, and loci still remain that have only one EMS allele. Further, the molecular identities of most of these *bus* loci remain unknown. Five of the 20 loci had been identified in unrelated mutant screens and only 3 of these previously defined genes, *egl-5*, *sur-2*, and *srf-3*, have been cloned. Among the 15 novel *bus* genes identified, only 6 to date have been cloned (M. Gravato-Nobre, D. O'Rourke, F. Partridge and J. Hodgkin, unpublished results).

Although many mutants were recovered after *mut-7*-induced Tc transposon mutagenesis, we found that these *bus* mutants were not readily identified through Tc1 insertion analysis using transposon insertion display (TID) (Wicks *et al.* 2000). Although Tc1 transposons provide a molecular tag for their site of insertion, the Tc1 tags are not unique enough for the rapid detection of the insertion site because the *C. elegans* genome contains many of these elements. Further, the endogenous transposons induced to hop in the *mut-7* background include Tc3 and other Tc family members. Moreover, mutations induced by EMS or Tc family transposon insertions that result in abnormal but variable responses to the pathogen have been little characterized hitherto, owing to the greater difficulty of working with less penetrant phenotypes.

As a means of more rapidly cloning rectal infection response genes, we explored the use of the *Mos1* transposon mutagenesis tool (Bessereau *et al.* 2001; Williams *et al.* 2005). Since *Mos1* transposons are not endogenous elements in the *C. elegans* genome, the *Mos1* sequence provides a unique molecular tag that can be used to identify the site of insertion and hence any gene that it may be disrupting. Here, we describe the results of *Mos1* screens for mutants with altered response to *M. nematophilum* and discuss the distinctive properties of mutants in four different genes, which affect various steps in the process of infection and host reaction. We also discuss the effectiveness of *Mos1* mutagenesis as a forward mutagenesis technique for *C. elegans*.

MATERIALS AND METHODS

Strains and general techniques: *C. elegans* nematodes were cultured as published (Brenner 1974). The Bristol isolate N2 was used as the wild-type strain. Pathogen susceptibility assays to *M. nematophilum* were carried out on mixed bacterial lawns of *Escherichia coli* (OP50) with 10% *M. nematophilum* (MBL) plates (Gravato-Nobre *et al.* 2005). For analysis of the Dar/Bus phenotype single L4 worms were picked to MBL or *E. coli* plates (four plates each) and adult progeny were scored for tail swelling. Scores are given as percentages plus or minus standard deviation. Worms on MBL plates were grown at 25° except when working with mutant alleles that result in a temperature-sensitive dauer-constitutive phenotype such as alleles of *tax-4*, *tax-2*, and *daf-11*. The pathogen response for these mutants was assayed at 20°. The following mutations and strains were used or generated in this study [unless otherwise noted, strains were obtained from the Caenorhabditis Genetics Center (CGC) and are described in WormBase at http://www.wormbase.org/]:

LGI: *tax-2(p691, p694, p671) (ky139)* (provided by C. Bargmann).
LGII: *tag-175(gk278)* (generated by the International *C. elegans* Gene Knockout Consortium, http://www.celeganskoconsortium.omrf.org).
LGIII: *tax-4(e2861)* (this study), *(ks11, ks28)* (provided by I. Mori), *daf-2(e1368, e1370)*, *daf-16(m26, mgDf50)*.
LGIV: *him-8(e1489)*.
LGV: *egl-8(e2917)* (this study), *(n488)*, *bus-19(e2912, e2964, e2965, e2966)* (this study), *unc-42(e270)*, *him-5(e1490)*, *daf-11(m47)*, *dpy-11(e224)*.
LGX: *bus-17(e2923)* (this study), *(e2800, e2695)* (Gravato-Nobre *et al.* 2005), *(br2)* (provided by C. Darby), *(cxTi9043)* (provided by L. Segalat, NemaGENETAG Consortium).

Mapping of single-nucleotide polymorphisms (SNP) was carried out using the *C. elegans* Hawaiian isolate CB4856 (Wicks *et al.* 2001). For *Mos1* mutagenesis we used the array-containing strains EG1470 *oxEx229[Mos1;myo-2p::GFP]* and EG2474 *oxEx166[hspp::Mos1Transposase;unc-122p::GFP;lin-15(+)]* (Bessereau *et al.* 2001). *him-8(e1489); oxIs12[unc-47p::GFP; lin-15(+)]* was used for outcrossing *tax-4(e2861)*. *him-8(e1489); bgIs312* [a transgene expressing green fluorescent protein (GFP) in the excretory cell, kindly provided by T. Bogaert] was used to outcross *bus-19(e2912)*. The deletion in *tag-175(gk278)* was verified by PCR on pooled lysates of mutants using GGAATGGACAAGCAAGGAAA and GACAGTTGGGTC GCTGATTT, primers that flank the deletion, and TCGGTTAAG AGGCTTTGTTG, a primer that is predicted to lie in the deleted area. OP50-GFP was obtained from the CGC.

Mutagenesis: *Mos1* mutagenesis was performed as published (Williams *et al.* 2005), using the extrachromosomal arrays *oxEx166*, which carries the *Mos1* transposase under the control of a heat-shock promoter, and *oxEx229*, which carries multiple copies of the substrate *Mos1* transposon. To facilitate construction of hermaphrodites carrying both arrays, in most of the selections EG1470 and EG2474 hermaphrodites were crossed with *him-8(e1489)* to generate strains that continually segregated array-carrying males. For each mutagenesis round, fresh double-array-carrying animals were generated. *him-8(e1489);oxEx166* males or *him8(e1489);oxEx229* males were crossed to L4 hermaphrodites carrying the other array. Progeny containing both arrays, recognized by the concurrent expression of GFP in the pharynx (*myo-2p::GFP*, contained in *oxEx229*) and GFP in the coelomocytes (*unc-122p::GFP*, contained in *oxEx166*), were propagated for three to six generations before heat-shocking. Double-transgenic animals were heat-shocked for 1 hr at 33°, 1 hr at 20°, and 1 hr at 33° and then allowed to recover overnight at 15° or 20° before picking onto MBL plates. Eggs from P_0's were collected 12–40 hr after heat shock. Five to 10 young adult F_1's were moved to MBL plates. Bus worms were selected in the F_2 generation. From each Bus F_2 4 F_3's were picked to a MBL plate and rescored for bacterial resistance. Worms that continually produced Bus mutants were kept for further analysis. Hop rates were determined as outlined in Williams *et al.* (2005). Worm lysates were made from single worms in 2.5 μl or five worms in 10 μl lysis buffer as published with the additional step of freezing on dry ice and/or at −70° for at least 20 min before incubation at 60° (Wicks *et al.* 2001).

Mutants that lost the extrachromosomal *Mos1*-bearing array were outcrossed at least once before assaying for the presence of *Mos1* elements and trying to locate the site of insertion

(unless noted). For those mutants that still contained a *Mos1* element, we determined the insertion site through inverse PCR on worm lysates as published (Bessereau *et al.* 2001). To identify *Mos1* insertion sites, inverse PCR (iPCR) was performed on *e2861* worm lysates digested with *Hae*III or *Sau*3A, *e2912* worm lysates digested with *Hae*III or *Mse*I, and *e2917* and *e2923* worm lysates digested with *Hae*III or *Alu*I. iPCR products were gel purified and then TA cloned using a TOPO-TA cloning kit (Invitrogen, San Diego). Products were amplified directly from colonies that were positive for transformation using oJL115/oJL116 and sequenced with oJL115. Sequences were considered true insertion flanking sequence if they contained the 5′ end of the *Mos1* element adjacent to the *C. elegans* genomic sequence starting at a TA dinucleotide. Primers used to amplify flanking regions of *Mos1* insertions are as follows: *egl-8* (B0348.4), TGCCGAAAGTTATCAAAAAGTTA and GCCAGATAACGCCTCAGAAG; *tax-4* (ZC84.2), TCGGAATTGTCTGGAAAGAAC and CTCACTCGGGTAAGCTCTGC; *bus-17* (ZK678.8), CAAAAAGATCACCGCCAAAA and CCCCATCTTTGGAGAGAACA; and *bus-19* (T07F10.4), ATGCCCTCCAACTTATCCTCTTG and TGCTTAACTTCTGCACATAGCACC.

EMS mutagenesis: To isolate more alleles of *bus-19*, N2 males were mutagenized with EMS as published (Brenner 1974). Mutagenized N2 males were mated to *bgIs312; unc-47(e270) bus-19(e2912)* hermaphrodites on MBL and allowed to mate overnight. Mated animals were then transferred once to a new MBL plate. In total, 6062 F_1's were scored for the Bus phenotype. Non-Unc F_2 Bus progeny were picked to new MBL plates and were scored for Bus non-Unc. Four F_2's bred true for the nonUnc Bus phenotype and were subsequently tested for the presence of the parental *Mos1* insertion, to preclude recovery of a recombinant carrying the original allele rather than a novel EMS mutation. One of these lines was a recombinant on the basis of the ability to amplify *Mos1* and flanking sequence of the array.

SNP mapping: We used SNPs to map the mutants to a linkage group (Wicks *et al.* 2001). CB4856 Hawaiian males were mated to mutant strains and F_1's were singled to MBL plates. Bus F_2's were used for snipSNP mapping alongside the original Bus homozygotes and CB4856 worms as controls. Primers and SNPs used for this linkage analysis are available on request.

Transgenic experiments: Transformation through microinjection was performed as published (Mello *et al.* 1991). For indicating successful transformation, we co-injected plasmids pRF4 *rol-6(su1006)* (Mello *et al.* 1991) or pPD97/98 *unc-122p::GFP* (a coelomocyte marker, gift of P. Sengupta), at 30 ng/μl while pTG96 *sur-5p::GFP* (Yochem *et al.* 1998) was injected at 40–50 ng/μl. Rescuing DNA and reporter constructs were injected at concentrations between 10 and 30 ng/μl. *tax-4(e2861)* mutants were rescued and analyzed using [*tax-4::GFP*] and [*odr-4p::tax-4::GFP*] constructs (kindly provided by M. de Bono).

For *bus-17* rescue experiments, cosmid ZK678 with *unc-122p::GFP* was injected into *e2923* and *cxTi9043* worms. We also amplified a 10-kb product from genomic DNA that extended from the last intron of the adjacent 3′ *wrt-4* ORF to the last intron of Y7A5A.1 residing 5′ of ZK678.8. This product was co-injected with *unc-122p::GFP* into *e2923* or *cxTi9043* homozygotes. In all of these experiments, lines were established on *E. coli* before testing transformants on MBL.

For *bus-19* rescue experiments, *him-8(e1489);lon-3(e2175)* lines were established with arrays containing cosmid T07F10, cosmid R90, cosmids T07F10 and R90, fosmid clone WRM0640cD03, a 7.3-kb fragment amplified from fosmid clone WRM0623dE01, or a 13-kb fragment amplified from fosmid clone WRM0623dE01 and co-injection markers *sur-5p::GFP* or *unc-122p::GFP*. Fosmid clones were provided by J. Perkins and D. Moerman. These lines were obtained either through mating with N2 lines containing the arrays or through direct injection of *him-8(e1489);lon-3(e2175)* animals. Lon males carrying each array were crossed to *bus-19(e2912)* or *bus-19(e2964)* homozygous animals and F_1's were transferred to MBL plates. Bus worms and Dar worms were scored for the presence of the GFP-expressing array.

Molecular analysis of *bus-17*: *bus-17* was amplified from N2-derived cDNA, which was prepared using RETROscript (Ambion, Austin, TX) following the manufacturer's recommendations. Primers ATCGTCGTCAGGTACTGTGTG with CCCCATCTTTGGAGAGAACA or TGAGACGTCGGAAACATGAA were used to amplify a 600- and a 1200-bp product, respectively, from cDNA template.

Molecular analysis of *bus-19*: T07F10.4a and T07F10.4b were amplified and sequenced from cDNA clones yk1387f02 and yk1345b03, kindly provided by Y. Kohara. Primers are available on request. To identify the mutations in *bus-19* EMS alleles, all exons and introns of T07F10.4 were sequenced from PCR-amplified genomic DNA (primer sequences are available on request). These products were sequenced on an Applied Biosystems (Foster City, CA) 3730xl DNA analyzer using Applied Biosystems Big Dye terminators.

Fluorescent staining and gross cuticle analysis: To visualize bacteria associated with infected worms, we incubated worms with the fluorescently labeled dye SYTO 13 (Invitrogen) as published. Bleach sensitivity assays and lectin staining were carried out as published. (Nicholas and Hodgkin 2004; Gravato-Nobre *et al.* 2005).

Behavioral assays: The bacterial choice assay was performed as published except that standard NGM were seeded with 40 μl of *E. coli* and 40 μl of *M. nematophilum* (Bargmann *et al.* 1993; Pujol *et al.* 2001). Plates were incubated overnight at 37° and cooled to room temperature before adding worms that had been grown on *E. coli*. These assays were performed at room temperature. We assessed the Skiddy (Skd) phenotype of *bus-19* alleles by placing 10 young adult animals, spaced apart from one another, at the edge of a bacterial lawn and letting them crawl into the lawn. As soon as a worm traversed the lawn it was removed from the plate and the tracks were qualitatively scored as wild type or Skd.

RESULTS

Isolation of *Mos1* insertion mutants: From a series of six small *Mos1* mutagenesis experiments, >7600 F_1 progeny from heat-shocked hermaphrodites carrying the two arrays that are jointly needed for *Mos1* mutagenesis (Williams *et al.* 2005) were collected and placed onto MBL containing 90% *E. coli* and 10% *M. nematophilum* and their progeny were examined for Bus (nonswollen) mutants (Table 1). From among the candidates picked, four *Mos1*-positive mutants exhibited a completely or largely penetrant Bus phenotype, while a fifth stable *bus* mutant did not carry a *Mos1* insertion. The *bus* mutation in this strain, *e2913*, was found to be an allele of a known gene, *bus-2*. Overall, the *Mos1* insertion rate into the genome was low (Table 1). However, the screening for loss of swelling and, in some cases, enhanced growth on pathogenic bacterial lawns allowed Bus mutants to be easily identified, such that screening large numbers of genomes was readily feasible.

To identify the insertion site in the *Mos1*-containing strains, iPCR was performed on lysates of the mutant

TABLE 1

Results of individual *Mos1* screens and hop frequencies

Screen	Transposition frequency (%)	No. of F_1's	Bus allele	Notes
1	ND	1061	*e2861*	More than one *Mos1* insertion.
2	20/57 (35)	930	*e2912*	More than one *Mos1* insertion.
3	1/14 (7)	1977	*e2913*[a]	No *Mos1* insertion.
4	33/73 (45)	1810	*e2917*	Only one insertion.
5	1/25 (4)	973	*e2923*	Only one insertion.
6	11/23 (48)	869		No Bus mutant found.
Total		7620		

The transposition frequency was measured as the percentage of progeny from heat-shocked double-transgenic animals that carry at least one *Mos1* insertion (Williams *et al.* 2005). To measure the transposition frequency, F_1 animals were picked blind from the progeny of heat-shocked double-transgenic P_0's. For each F_1 that had lost the *Mos1* substrate array 5–10 F_2 animals were tested by PCR for the *Mos1* element. For each F_1 that still carried the array, non-array-carrying F_2 progeny were identified and F_3 animals were tested for *Mos1* insertions.

[a] *e2913* did not complement *bus-2*. As we already had a number of alleles of *bus-2*, and this strain did not contain a *Mos1* insertion, we did not keep this allele for further analysis.

worms. In each case, a *Mos1* insertion was identified in the coding region of a unique ORF. *Mos1* insertions were identified in exon 2 of *egl-8* (B0348.4), exon 4 of *tax-4* (ZC84.2), and exon 2 and exon 1 of two uncharacterized ORFs, ZK678.8 on LGX and T07F10.4 on LGV, respectively (Figures 1 and 2). The close proximity and similar phenotypes of *e2923* mutants to *bus-17* mutants isolated previously suggested that *e2923* might be an allele of *bus-17*. *e2923* does not complement *bus-17(e2800)*, confirming this locus assignment. Two of the four mutants, *tax-4* and *bus-19*, had more than one insertion in their genome; however, these insertions were not in coding regions and were verified as irrelevant after loss of the insertions through outcrossing and/or mapping the Bus phenotype (see below).

Comparison of bacterial adherence of *bus* mutants: Unlike several lethal pathogens of *C. elegans*, *M. nematophilum* does not colonize the intestine of the worm; instead, the vital dye SYTO 13 reveals *M. nematophilum* colonization in the rectum of infected worms (Gravato-Nobre *et al.* 2005) (Figure 3). This colonization correlates with tight adherence of the bacteria as shown by close examination of infected and extensively washed worms (Hodgkin *et al.* 2000). On the basis of the level of bacterial colonization relative to wild-type infected worms, the *bus* mutants isolated in previous screens were broadly classified into four groups (Gravato-Nobre *et al.* 2005). The mutants identified here also exhibit a range of rectal colonization by *M. nematophilum* (Figure 3). In particular, *egl-8(e2917)* mutants exhibit SYTO 13 bacterial staining in the distal portion of the rectum. This suggests that *egl-8* is not required for the adherence of the pathogen and may therefore play a role in the postadherence swelling response. *tax-4(e2861)* mutants also exhibit bacterial staining; however, this staining is not consistent and is correlated with the presence of a Dar response. Although *tax-4(e2861)* mutants are sometimes Dar, many worms exhibit strongly attenuated swelling or are completely Bus with little or no rectal staining. No mutants reported in previous Bus screens share these exact characteristics; however, mutants that exhibit significant variability in Dar response have been little analyzed so far. The *tax-4(e2861)* mutation does not appear to affect the postadherence swelling response; instead, *tax-4* wild-type activity appears to be variably required for the bacteria to efficiently establish a rectal infection.

The other two mutants resembled the majority class of *bus* mutants isolated in previous screens, in that they do not exhibit any bacterial colonization and are 100% Bus. *bus-17* alleles isolated in the previous screen fall into this category, as does *e2923*, the *bus-17* allele isolated in this screen. Similarly, *bus-19(e2912)* mutants were invariably Bus and did not exhibit any rectal SYTO 13 bacterial staining. These observations suggest that *bus-17* and *bus-19* are required for bacteria to adhere to the rectal and postanal cuticle.

Cuticular defects of *bus* mutants: The failure of bacteria to adhere to the rectal epithelium of *bus-17(e2923)* and *bus-19(e2912)* mutants may be due to alterations of the cuticle. A subset of the *bus* mutants previously identified did not show any rectal colonization of *M. nematophilum* and was demonstrated to have altered surface properties (Gravato-Nobre *et al.* 2005). Alterations in the surface properties of the worm can be observed by staining worms with labeled lectins such as Concanavalin A (ConA), wheat germ agglutinin (WGA), and soybean agglutinin (SBA) (Link *et al.* 1992). We examined *bus-17(e2923)* and *bus-19(e2912)* mutants for lectin binding and observed that these mutants exhibited strong lectin binding across the surface of the worm, in contrast to a lack of lectin binding by wild-type worms (Figure 4, A and C). The larvae of both *bus-17* and *bus-19* worms also exhibited significant levels

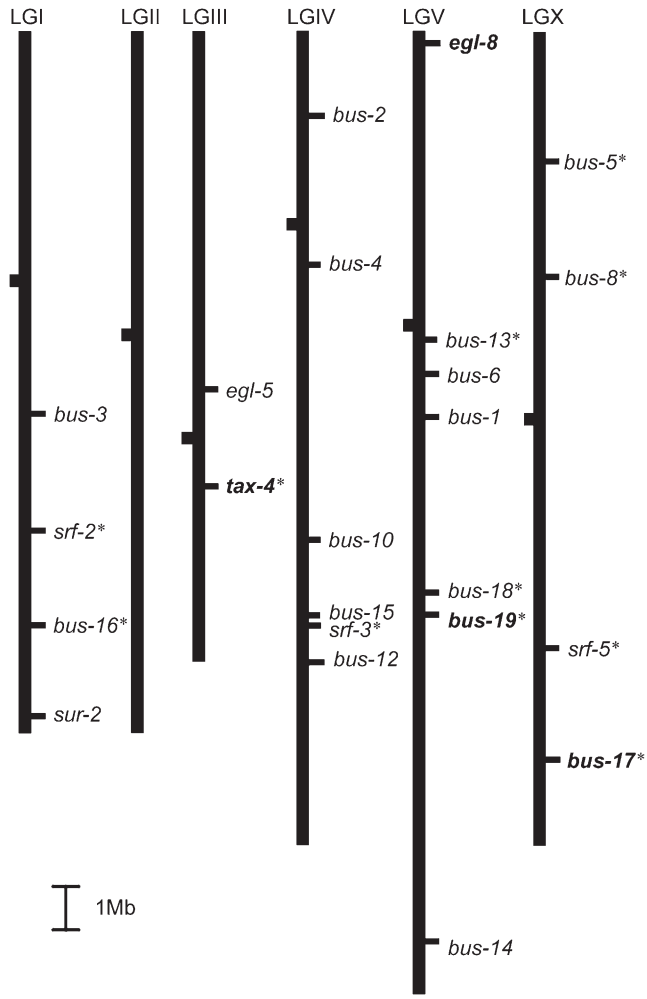

FIGURE 1.—Genetic map of *bus* loci recovered from selections and screens for resistance to infection by *M. nematophilum* bacteria. The map has been scaled to the genome sequence. Alleles of genes shown in boldface type were identified in the present *Mos1* mutagenesis selection. Alleles of other genes were identified in previous EMS and *mut-7* screens, including *bus-17* (GRAVATO-NOBRE *et al.* 2005). *bus-17* and *bus-19* were cloned in this study. The asterisk indicates that fluorescently labeled lectins bind these mutants.

of lectin binding, in some cases with severe disruptions in staining, signifying areas of the cuticle that had been physically damaged.

bus-17 and *bus-19* exhibit a Skiddy (Skd) phenotype, an apparent loss of traction on the agar plate, which results in a characteristic high-frequency wave pattern in the bacterial lawn (Figure 4B). The Skd phenotype has been noted for many of the previously identified *bus* mutants including *srf-3*, *bus-16*, *bus-17*, and *bus-18* (GRAVATO-NOBRE *et al.* 2005). *bus-19* mutants have more severe cuticle defects than *bus-17* mutants. We observed that *bus-19* mutants have disrupted alae, lateral ridges that run the length of the adult cuticle. ConA staining revealed the alae of wild-type worms as well as the *bus* mutants (this staining is most likely due to the trapping of the labeled lectin in the ridges). Although alae are distinct in wild type, *bus-17*, and *srf-3*, clearly demarcated lateral ridges in *bus-19* mutants are not present. The fact that alae are present in *srf-3* and *bus-17* suggests that the Skd phenotype is not likely to be due to defects in these structures and that traction relies on other surface properties of the worm.

tax-4(e2861) mutants exhibited cuticle defects and lectin binding as well, but the lectin staining correlated with areas of the worm that had accumulated extra cuticle and may therefore be a result of trapped lectins rather than breaches in the cuticle (Figure 5). Further, the staining was localized to the anterior region of *tax-4* mutants rather than along the whole body as observed for other *bus* mutants.

***egl-8(e2917)*:** *egl-8(e2917)* mutants grow very slowly on MBL plates and are severely constipated (Con). On *E. coli* alone, these mutants exhibit visible egg-laying defective (Egl) and Con phenotypes. We identified only one *Mos1* insertion in unoutcrossed mutants, which was an insertion in exon 2 of *egl-8* (Figure 2); in further outcrosses the Bus phenotype cosegregated with the *Mos1* insertion in *egl-8*. *egl-8* encodes the β-subunit of phospholipaseC (PLCβ), which catalyzes the cleavage of phosphatidylinositol 4,5-bisphosphate (PIP_2) into inositol 1,4,5 triphosphate (IP_3) and diacyl glycerol (DAG), which are critical second messengers in cell signaling pathways (LACKNER *et al.* 1999; MILLER *et al.* 1999). EGL-8 is characteristic of the PLCβ family members in that it contains an N-terminal pleckstrin homology (PH) domain, an EF hand calcium-binding repeat region, X and Y catalytic domains, a C2 lipid-binding domain, and the $G_q\alpha$-interacting G box (JAMES and DOWNES 1997). The *egl-8(e2917)* insertion is predicted to disrupt the PH domain, which is required for binding to PIP_2. This insertion would presumably affect all transcripts of *egl-8* and is likely to be a null. We compared *egl-8(e2917)* mutants with worms homozygous for the *egl-8(n488)* null allele. *egl-8(n488)* mutants are also Bus, grow very slowly, and are severely Con on MBL. Further, *egl-8(e2917)* does not complement *egl-8(n488)* for the Bus phenotype. *M. nematophilum* bacteria adhere to distal rectal epithelium of both *egl-8(e2917)* and *egl-8(n488)* mutants but fail to elicit the swelling response (Figure 3). These mutants are severely Con so it is conceivable that the pressure inside the distended gut may force bacteria into the rectum and that bacteria leaked into the rectum may not be distinguishable from adherent bacteria by the SYTO 13 dye. However, this scenario is unlikely as *egl-8* mutants fed *E. coli* OP50-GFP (*E. coli* expressing GFP), are also Con but do not exhibit patches of fluorescence in the rectum like that exhibited with SYTO 13-stained worms infected with *M. nematophilum* (data not shown). These observations imply that bacterial attachment factors are still present in these mutants and that the inability to swell in the presence of *M. nematophilum* is likely due to a defect in signaling the swelling response upon infection.

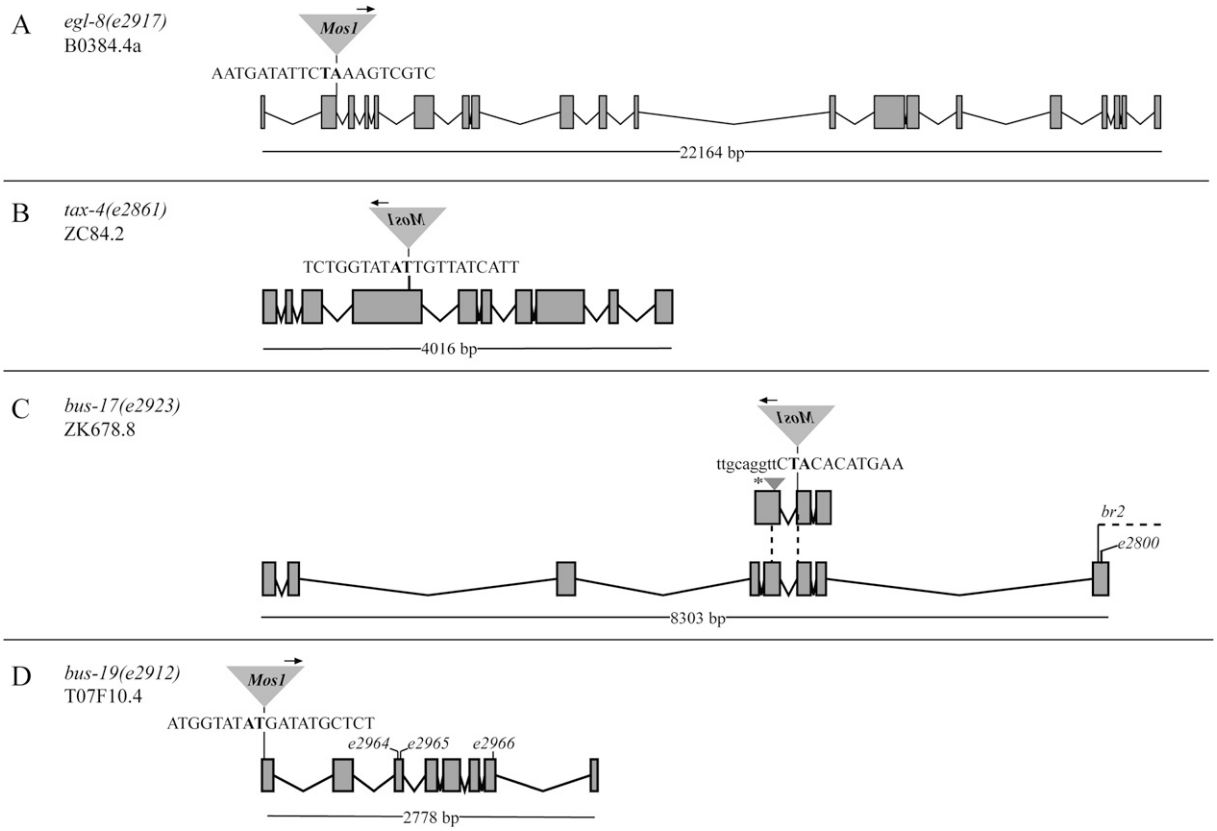

Figure 2.—Insertion sites and polarities of *Mos1* elements in *bus* mutants. Arrows above the *Mos1* elements indicate the orientation of the *Mos1* primer oJL115 used for sequencing iPCR products of mutant lysates. Uppercase letters signify exonic sequence. Gene models are taken or modified from WormBase Release WS154. The gene models are not drawn to scale with each other; the length of the ORF, however, is noted below each model. (A) *egl-8(e2917)* mutants have a *Mos1* insertion in the second exon of B0384.4. This insertion would affect all three alternatively spliced transcripts, a, b, and c, of *egl-8*; only the B0384.4a transcript is modeled here. (B) *tax-4(2861)* mutants have a *Mos1* insertion in the fourth exon of ZC84.2. (C) *bus-17(e2923)* mutants have an insertion in exon 2 of the WormBase (release WS154) ZK678.8 gene model (top gene model). This insertion site corresponds to exonic sequence of the sixth exon of a TWINSCAN prediction for the gene (bottom gene model). The arrowhead (asterisk) designates a *Mos1* insertion in *cxTi9043* mutants, which was generated by L. Segalat. The dotted lines indicate the positions of the *Mos1* insertions in the corresponding TWINSCAN prediction. The *br2* lesion is a 311-bp deletion that would affect the 3′ end of the *bus-17* coding sequence, as denoted by the dotted line. The *e2800* mutation is a missense mutation; see text and Figure 6 for more information. (D) *bus-19(e2912)* mutants have a *Mos1* insertion in the first exon of T07F10.4. *e2964*, *e2965*, and *e2966* are missense alleles of *bus-19* that were isolated in this study.

***tax-4(e2861)*:** We identified three *Mos1* insertions in a 2×-outcrossed version of *e2861* Bus mutants. Two of these insertions were in intergenic regions on LGV, while a third insertion was in the fourth exon of ZC84.2 on LGIII, which encodes *tax-4*. We determined that the insertion of *Mos1* in *tax-4* was probably the relevant mutation by finding tight snpSNP linkage of *e2861* to a Bristol polymorphism in F10E9, close to *tax-4* on LGIII. As noted above, mutants homozygous for *e2861* exhibit variability in their response to *M. nematophilum*. At 20°, a majority of the animals examined exhibited no or very slight swelling of their postanal region, but almost half (48 ± 8%, $N = 175$) of the population is Dar (distinctly swollen). Under the same 20° conditions, most N2 wild-type worms (81 ± 1%, $N = 512$) exhibited a Dar response. The strength of the *tax-4(e2861)* Dar response correlates with increased bacterial colonization, as shown by staining with SYTO 13 (Figure 3). We also looked at other *tax-4* mutants and found that homozygous mutants of two other alleles of *tax-4*, *ks11* and *ks28*, exhibited a variable Bus phenotype similar to *e2861*; for example, only 52 ± 10% ($N = 311$) of the *tax-4(ks11)* population was Dar when grown on MBL plates.

The TAX-4/TAX-2 cyclic nucleotide gated channel is required in a subset of neurons for full susceptibility to *M. nematophilum*: *tax-4* encodes the homolog of the cyclic nucleotide-gated (CNG) channel α-subunit (Komatsu *et al.* 1996). TAX-4 forms a channel with TAX-2, a homolog of the CNG channel β-subunit (Coburn and Bargmann 1996; Komatsu *et al.* 1999). TAX-4 and TAX-2 overlap in expression in 11 neurons and are responsible for modulating many behaviors of the worm, including chemosensation (to both soluble and volatile compounds), thermosensation, dauer formation, and social aggregation (Dusenbery *et al.* 1975; Hedgecock and Russell 1975; Bargmann and Horvitz 1991a,b;

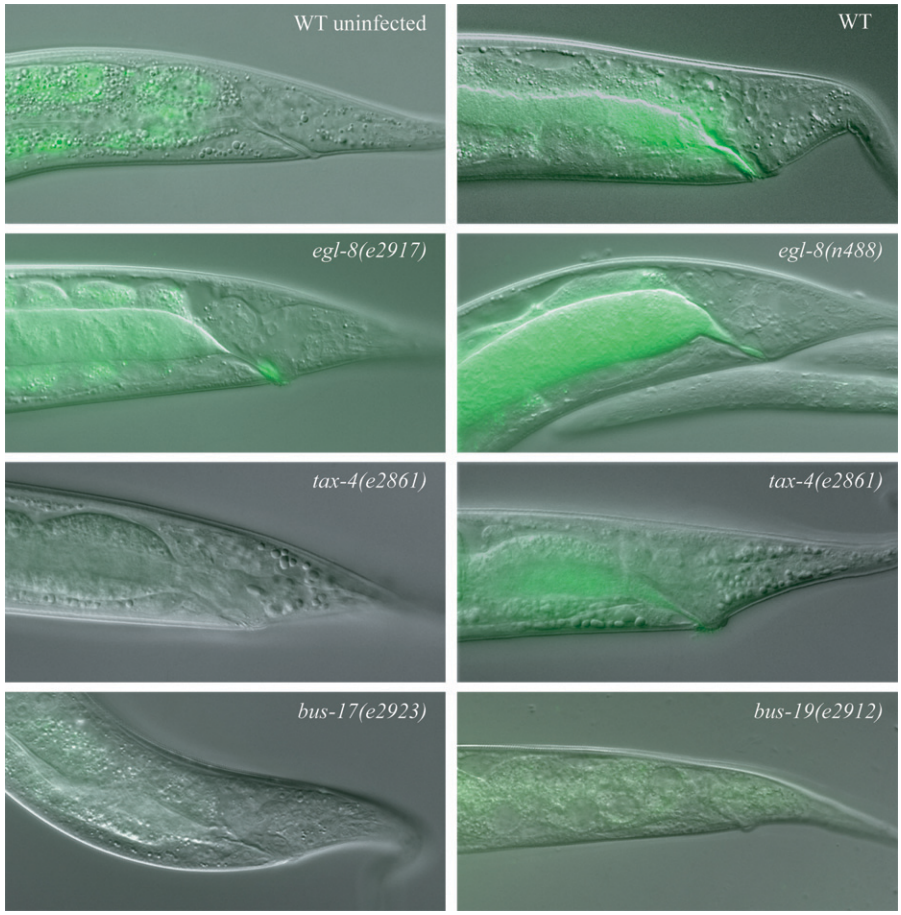

Figure 3.—The swelling response to *M. nematophilum* is attenuated or absent in Bus mutants. *M. nematophilum* causes a *d*eformed *a*nal *r*egion (Dar) phenotype on infected WT worms. *M. nematophilum* adheres tightly to the rectal epithelium of WT worms and colonized the rectum as visualized by SYTO 13. *egl-8(e2917)*, *tax-4(e2861)*, *bus-17(e2923)*, and *bus-19(e2912)* mutants do not swell in the presence of *M. nematophilum* and all mutants except *egl-8* have a loss or attenuation of rectal colonization by the bacteria. Bacteria still colonize the rectum of *egl-8* mutants *e2917* and *n488*, the canonical null allele. *tax-4* mutants exhibit variability in response to infection.

Bargmann *et al.* 1993; Komatsu *et al.* 1996; de Bono *et al.* 2002; Satterlee *et al.* 2004). Further, the TAX-4/TAX-2 channel acts downstream of the DAF-11 guanylate cyclase in many chemosensory behaviors and in dauer formation (Birnby *et al.* 2000). To test if the action of the channel is required for the swelling response, we exposed *tax-2* and *daf-11* mutants to the pathogen. Like *tax-4(e2861)* and *tax-4(ks11)* mutants, *tax-2(p671)*, *tax-2(p691)*, *tax-2(ky139)*, and *daf-11(m47)* homozygotes are all variably Bus (Figure 5A). Surprisingly, *tax-2(p694)* worms were strongly Dar (100%, $N = 124$) whereas only 51 ± 10% ($N = 131$) of *tax-2(p671)* mutants were Dar. *tax-2(p694)* mutants carry a mutation that deletes the first exon of *tax-2*, resulting in altered expression of *tax-2* and presumably a shorter TAX-2 product (Coburn and Bargmann 1996). This deletion in *tax-2* has been demonstrated to affect TAX-2 function only in a subset of the neurons that require the TAX-4/TAX-2 channel (Coburn and Bargmann 1996). Specifically, the *p694* deletion does not affect the expression or function of *tax-2* in six amphid neurons, AWB, AWC, ASG, ASI, ASK, and ASJ. These neurons mediate chemosensation (AWB, AWC), taste (ASG, ASK), and dauer formation (ASI, ASJ). The fact that *tax-2(p694)* worms have a strong Dar response, whereas other *tax-2* mutants are variably Bus, implicates one or more of these six amphid neurons in susceptibility to *M. nematophilum*.

TAX-4 mediates a choice between bacterial foods: A possible explanation for the implication of *tax-2* and *tax-4* in the infection of worms by *M. nematophilum* is that these *tax* mutants are altered in their exposure to the pathogen, as a result of aberrant taxis behavior. *C. elegans* has been shown to be able to recognize and avoid other pathogens (Pujol *et al.* 2001). We therefore compared behavioral parameters between wild-type and mutant worms. Wild-type worms tend to avoid lawns contaminated with *M. nematophilum*. By contrast, *tax-4(e2861)* mutants can be found equally distributed inside and outside a mixed bacterial lawn. Mutants carrying a strong allele of *tax-2*, *p671*, displayed a comparable response to *tax-4(e2861)* (Table 2). When we challenged the worms with a direct choice between *E. coli* and *M. nematophilum* as a food source we found that wild-type worms exhibited a strong preference for *E. coli*. *tax-4(e2861)* mutants, however, exhibited no preference for one bacterium over the other (Figure 5B). *tax-2(p694)* mutants behaved like wild-type worms and exhibited a preference for *E. coli*. Comparable results were obtained in experiments using two Pseudomonas strains that are toxic to both wild-type and *tax-4* mutant *C. elegans*, indicating that the defective avoidance behavior of *tax-4* is

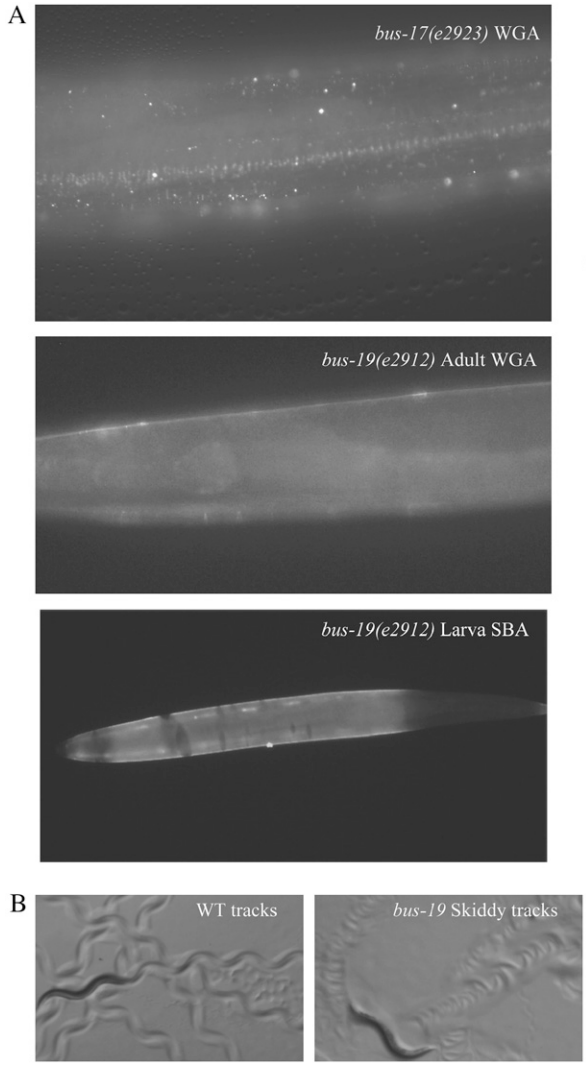

Figure 4.—Skiddy (Skd) phenotype and cuticle defects of *bus* mutants. (A) Fluorescently labeled lectins bind to *bus-17* and *bus-19* mutant cuticles. Mutants were stained with WGA or SBA. Wild-type worms (not shown) do not exhibit cuticle lectin binding of WGA or SBA. (B) The Skd phenotype is characterized by a loss of traction on the agar. Wild-type worms propel themselves forward with little slippage, and each body bend leaves a characteristic wave pattern behind (left). *bus* and *srf* mutants are unable to propel themselves forward as easily as wild-type worms, which results in a high-frequency wave pattern in the food (right). (C) Alae, revealed by Concanavalin A (ConA) fluorescence, exhibit abnormalities in *bus-19* mutants.

general, rather than a result of its resistance to *M. nematophilum* (G. Preston and J. Hodgkin, unpublished results). As noted above, *tax-2(p694)* mutants have normal chemotaxis and taste functions as well as normal dauer formation regulation. These results indicate a paradoxical situation for *tax-4* and *tax-2* mutants: the strong *tax* mutants do not avoid the pathogenic food as much as wild-type worms do, yet they end up less sickened by it.

TAX-4 and TAX-2 have been demonstrated to act downstream of DAF-11, a guanylate cyclase and group I dauer pathway gene (Thomas *et al.* 1993; Birnby *et al.* 2000). Like *tax-4(e2861)*, *daf-11(m47)* mutants exhibit attenuated swelling in the presence of *M. nematophilum*. *daf-11* mutants are abnormal in dauer formation and enter into dauer under nonpermissive conditions (Daf-c) at 25°, like most *tax-4* and *tax-2* mutants. In contrast, *tax-4* and *tax-2* mutants that do not have a Daf-c phenotype at 25° have a wild-type response to *M. nematophilum*, suggesting that defects in the entry or exit from the dauer state may be affecting the infection. However, activation or inhibition of the dauer program *per se* does not greatly alter the response of the worms to *M. nematophilum*. We assayed other dauer-regulation-defective mutants for the Dar response. Specifically, we tested both Daf-c mutants, *daf-2(e1368)* and *daf-2(e1370)*, and dauer-formation-defective (Daf-d) mutants *daf-16(m26)* and *daf-16(mgDf50)*. In addition to being Daf-c, *daf-2(e1368)* and *daf-2(e1370)* have recently been shown to exhibit increased resistance to killing by bacterial pathogens (Garsin *et al.* 2003). Specifically, *daf-2(e1370)* exhibited much stronger resistance than *e1368* to killing by these pathogens, although *e1368* still exhibited a marginal increase in resistance. *e1368* is a class 1 allele of *daf-2*, which encompasses the Daf-c(ts), increased adult life span (Age), and increased thermotolerance (Itt) phenotypes. Class 2 alleles, such as *e1370*, exhibit all these phenotypes in addition to exhibiting gonad abnormalities, embryonic and L1 arrest, diminished adult body size, reduced pharyngeal pumping, and uncoordinated movement (Gems *et al.* 1998). The Daf-c and Age phenotypes of both class 1 and class 2 alleles can be suppressed by mutations in *daf-16*. *daf-16* mutants are dauer defective and thus do not enter into or maintain the dauer state.

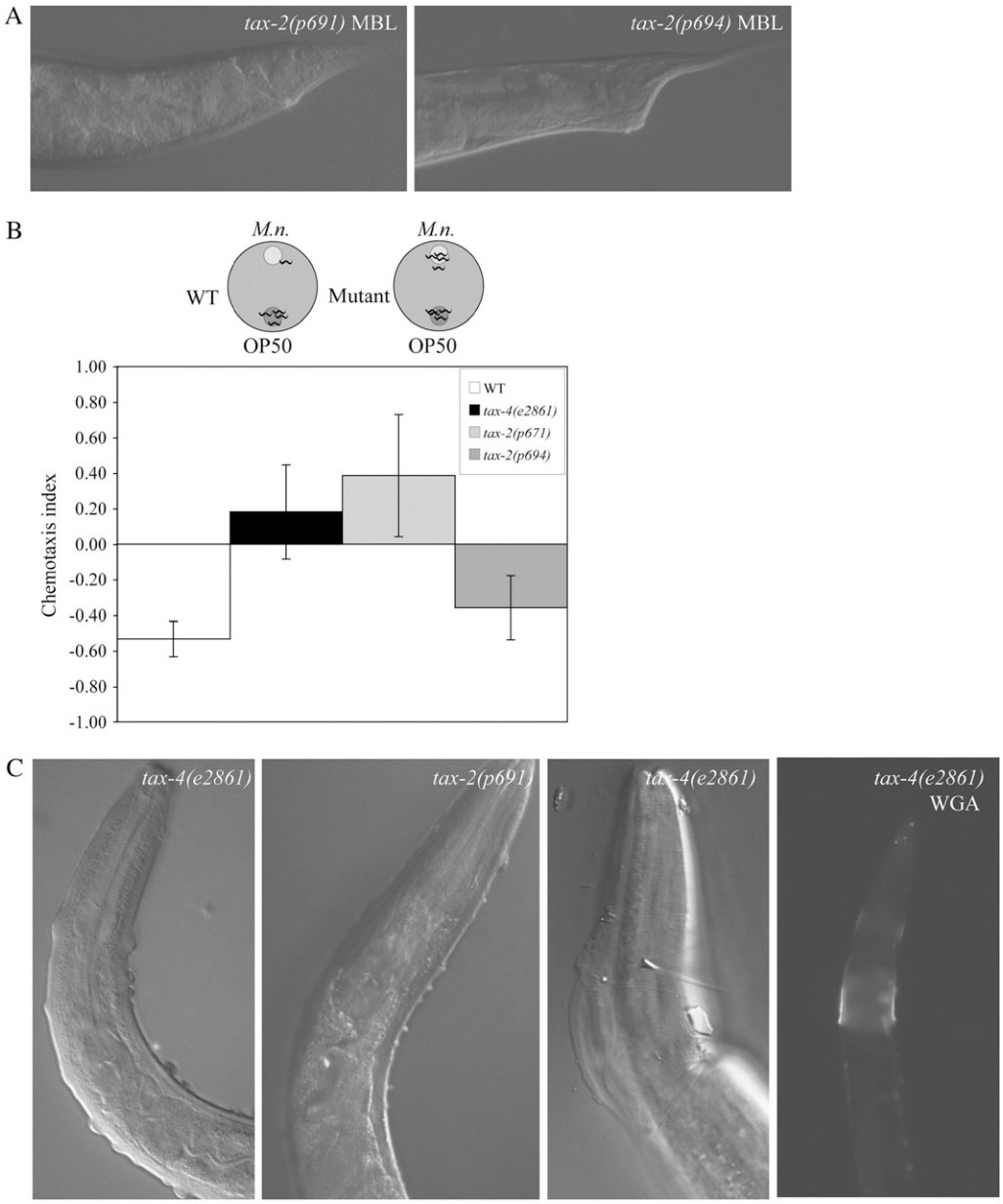

FIGURE 5.—Behavioral and cuticle defects of *tax-4* and *tax-2* mutants. (A) Different *tax-2* alleles exhibit varied responses to *M. nematophilum*. *tax-2(p691)* (left) is Bus like *tax-4(e2861)*, whereas *tax-2(p694)* (right) is Dar. (B) TAX-4 is required for the avoidance behavior to *M. nematophilum* and for cuticle integrity. Chemotaxis index = (no. worms at *M. nematophilum* − no. worms at *E. coli*)/total no. worms. WT, $N = 519$, six trials; *tax-4(e2861)*, $N = 444$, three trials; *tax-2(p671)*, $N = 154$, two trials; *tax-2(p694)*, $N = 653$, four trials). (C) *tax-4* and *tax-2* mutants exhibit cuticle defects when grown on *E. coli*, which include starvation-induced bumpy cuticles reminiscent of gherkins (left) and collars of extra cuticle, which can be highlighted by fluorescently labeled WGA lectin binding (right).

Because dauer larvae do not become Dar in the presence of the pathogen, we assayed *daf-2* mutants grown at 15° and shifted to 25° at L3, to avoid the temperature-sensitive Daf-c phenotype. We found that *daf-2(e1368)* mutants exhibited a normal Dar response to the pathogen after shifting to 25°. *daf-2(e1370)* mutants, on the other hand, exhibited a range of morphological phenotypes that prevent strong conclusions about the swelling response. In the case of *daf-16*, the inhibition of the dauer program does not alter the swelling response to the

TABLE 2

Fraction of animals in a population within a bacterial lawn

Genotype	*E. coli*	*M. nematophilum*	Trials
WT	0.71 (±0.09), $N = 34$	0.24 (±0.02), $N = 89$	2
tax-4(e2861)	0.72 (±0.08), $N = 39$	0.94 (±0.04), $N = 52$	3
tax-2(p671)	0.98 (±0.02), $N = 38$	0.94 (±0.06), $N = 32$	2

Two trials were performed for each bacterial lawn except in the case of *tax-4(e2861)*, where three trials were done. SEM is indicated in parentheses; *N*, total numbers of worms tested over all trials.

pathogen, as mutants homozygous for *daf-16(m26)* or *daf-16(mgDf50)* were 100% Dar as were wild-type worms at 25°.

***tax-4* cuticle defects:** We observed that *tax-4* and *tax-2* mutants exhibit cuticle defects that have not been reported before. These defects include an accumulation of cuticle around the pharyngeal area of adult worms, which is present at a low level in the population (<10%) and can be observed under the dissecting scope or by staining with fluorescently labeled WGA (Figure 5C). This extra cuticle is suggestive of a molting defect. Worms that have the collars of extra cuticle cannot be tested for the swelling response to *M. nematophilum* since they are already adults when the collar is formed. However, the collars have been noted on Bus and Dar worms grown on infected plates at 15°. Unfortunately the swelling response of wild-type worms at 15° is variable and often attenuated, so we cannot conclude if the *tax-4* mutants with molting defects are more or less susceptible to postanal swelling. In addition to these defects, *tax* mutant worms on starved plates exhibit an abnormal bumpy surface appearance, resembling a gherkin (Figure 5C), a phenotype that is not seen in starved wild-type worms. We interpret these observations to suggest that these mutants have subtle defects in their cuticles that impair initial bacterial adherence.

***bus-17(e2923)*:** *e2923* has a *Mos1* insertion in ZK678.8 on the right arm of LGX (Figure 2). The location of the mutation responsible for the Bus phenotype was confirmed by snipSNP linkage to the Bristol polymorphism in F23D12 on LGXR. Another *Mos1* insertion reported for ZK678.8, *cxTi9043*, was obtained from the *Mos1* insertion consortium (Granger *et al.* 2004). This mutant is also Bus and did not complement *e2923*. Both mutants were rescued by the ZK678 cosmid and by a 10-kb fragment amplified from wild-type genomic DNA. The 10-kb rescuing fragment encompasses ZK678.8 and extends to the last introns of the adjacent 5′ and 3′ genes. Two EMS alleles of *bus-17* (*e2695* and *e2800*) were identified in a previous screen for *bus* mutants (Gravato-Nobre *et al.* 2005). Due to the close proximity of *bus-17* to *e2923* and to the similarities in phenotypes between the mutants, *e.g.*, skiddiness and lectin binding, we performed a complementation test between these mutants. We found that *e2923* does not complement *bus-17(e2800)*. Two other alleles of *bus-17* were identified in the lab of Creg Darby in a selection for mutants resistant to the accumulation of Yersinia *sp.* biofilm (C. Darby, personal communication). *Yersinia pestis* and *Y. pseudotuberculosis* form a biofilm on the head of *C. elegans*, covering the mouth of the worm and causing death by starvation (Darby *et al.* 2002). Two *bah* (*b*iofilm *a*bsent from *h*ead) mutations, *br2* and *br11*, failed to complement *bus-17* for the Bus phenotype as well as for the Bah phenotype (C. Darby, personal communication).

BUS-17 is predicted to be a member of the glycosyl transferase 31 (GT31) family and is most closely related to the human β-1,3-*N*-acetylglucosaminyltransferase 5 (B3GNT5) (Figure 6). The predicted BUS-17 protein contains one conserved active site motif for this family but does not appear to have the DXD catalytic domain that is conserved in this family; instead an asparagine replaces the first aspartic acid, which is a mildly conserved substitution. The WormBase (release WS154) gene model of ZK678.8 predicted *bus-17* to encode a noncanonical galactosyltransferase, which lacked the characteristic transmembrane domain. A nucleotide Blast search against the *C. briggsae* genome using sequences 5′ and 3′ of the *C. elegans* WS154 gene model revealed highly conserved sequences in both regions of CBG07766, the *C. briggsae* ortholog of ZK678.8. While the similar 5′ regions could be explained as conserved promoter elements, the similar 3′ region had been annotated as a coding sequence in the *C. briggsae* ortholog, suggesting probable omissions in the WS154 *C. elegans* gene model. Further, no mutations in the WS154 ZK678.8 sequence were identified in any of the non-*Mos1* alleles of *bus-17*. Mutations in two of the alleles, *e2800* and *br2*, were subsequently found in the conserved 3′ region, further supporting a larger gene model for ZK678.8. The obsolete gene model predicted by TWINSCAN, with additional 5′ and 3′ exons, appears to better annotate the gene (Korf *et al.* 2001). Finally, we verified that this gene model is correct by amplifying and sequencing *bus-17* cDNA, which extended from within the first exon of the TWINSCAN prediction to the 3′-UTR.

BLASTX of the TWINSCAN prediction reveals an intact galactosyltransferase, which includes an N-terminal transmembrane domain as well as an additional C-terminal sequence, which is altered in mutants that carry the *bus-17(e2800)* or *bus-17(br2)* mutations (Figures 2 and 6).

***bus-19(e2912)*:** In addition to being Bus and Skd, *bus-19(e2912)* homozygous mutants are mild dumpy (Dpy), slow growing (Gro), hypersensitive to bleach, dauer defective (Daf-d), and segregate arrested larvae with rod-like lethality (<10%). Two *Mos1* insertions were identified in an outcrossed *bus-19(e2912)* mutant, one in exon 1 of T07F10.4 on LGV and another in an intergenic region upstream of F54F12.2 on LGIII. In further outcrosses, the Bus phenotype was found to segregate only with the T07F10.4 insertion. We rescued *bus-19* mutants with overlapping cosmids T07F10 and R90, but cosmid T07F10 alone did not rescue *bus-19(e2912)*. Since T07F10.4 is at the end of the cosmid, it was possible that the end of T07F10.4 was deleted from the cosmid. The overlapping cosmid, R90, is likely to include most or all of the T07F10.4 open reading frames; however, it was not able to rescue the Bus phenotype of *bus-19* mutants. Surprisingly, R90 did rescue the morphological Dpy and Skd phenotypes of *bus-19(e2912)*. The two cosmids together fully rescued all phenotypes. This suggests that part of *bus-19* is deleted from the T07F10 cosmid and that this missing region was

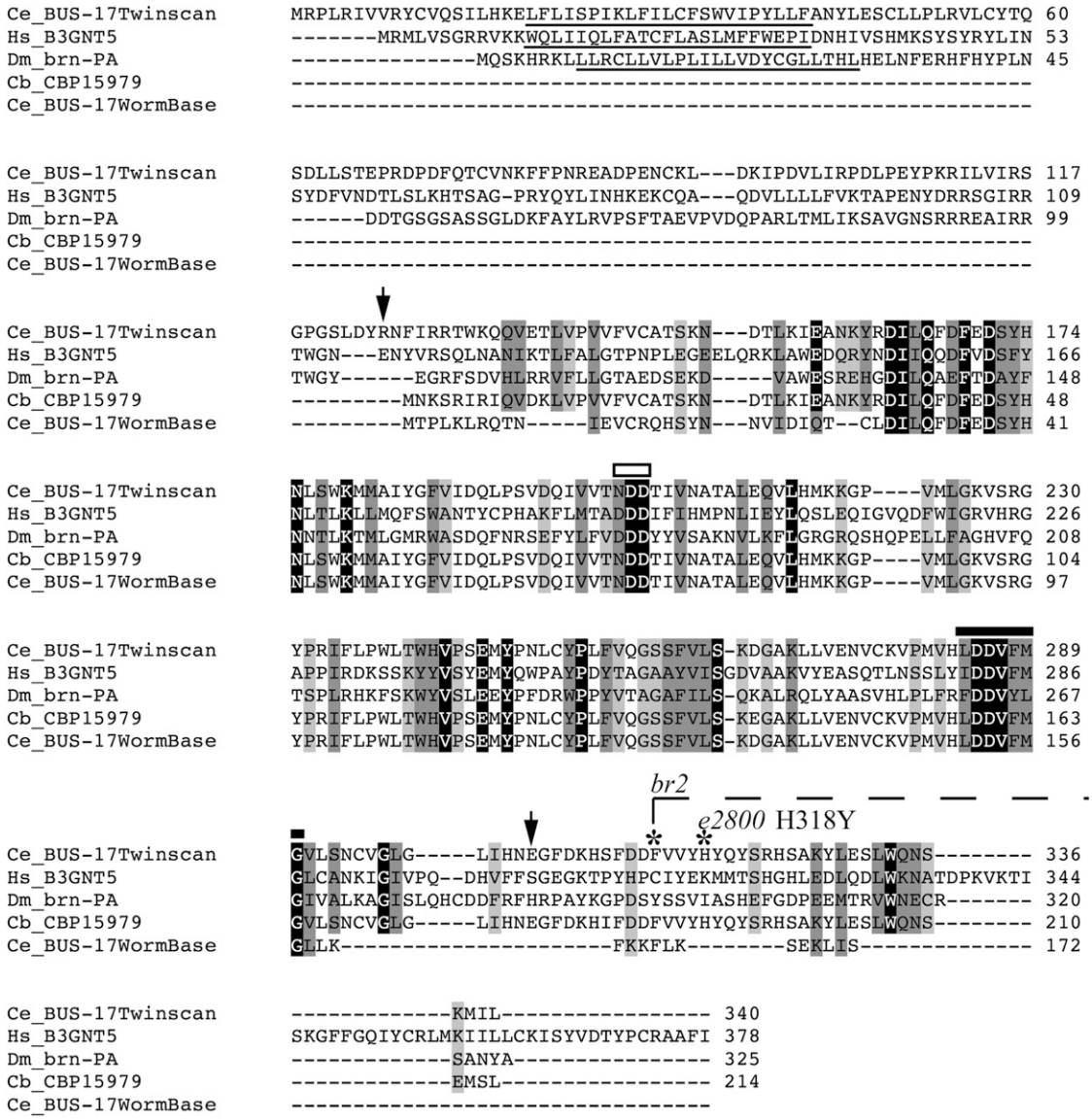

FIGURE 6.—ClustalW (v.1.83) alignment of BUS-17 with B3GALT family members. Light gray boxes signify semiconserved substitutions, dark gray boxes signify conserved substitutions, and black boxes signify identical residues. Species are as follows: *Cb*, *Caenorhabditis briggsae*; *Hs*, *Homo sapiens*; *Dm*, *Drosophila melanogaster*. Underlines denote TMHMM2 predicted TM domains for each protein. The boundaries of the BUS-17 pfam01762 galactosyltransferase domain are indicated by arrows. The DXD catalytic core motif (box) is characteristic for this family. BUS-17 and its *C. briggsae* ortholog have an N substitution of the first D. The N-terminal globular domain (thick line) is also conserved in family 31 galactosyltransferases. The *br2* deletion lesion begins at amino acid 314 and would affect the remaining BUS-17 protein. The amino acid change caused by *e2800* is noted. B3GNT5, β-1,3-*N*-acetylglucosaminyltransferase; Brn-PA, brainiac.

provided by the R90 cosmid. Alternatively, *bus-19(e2912)* could have been another very close mutation, which is not tagged by the *Mos1* transposon, but is responsible for the Bus phenotype. This possible scenario was supported by RNAi results in that knockdown of T07F10.4 in both N2 and *rrf-3* mutant worms phenocopies the Dpy and Skd phenotypes of *bus-19(e2912)*, but fails to phenocopy the Bus phenotype when the worms are exposed to *M. nematophilum*.

To clarify this situation, three more *bus-19* alleles, *e2964*, *e2965*, and *e2966*, were recovered in a noncomplementation screen for the Bus phenotype. *bus-19(e2964)* is the most similar of the three new alleles to *bus-19(e2912)*. *bus-19(e2965)* is variably Dpy but is a strong Bus mutant and is strong Skd. *bus-19(e2966)*, however, is non-Dpy, non-Skd, and only weakly Bus. The Bus phenotype is stronger in a *trans*-heterozygote, genotype *bus-19(e2912/e2966)* although such heterozygotes still exhibit weak swelling. As with *bus-19(e2912)* mutants, all mutants were rescued by the simultaneous introduction of T07F10 and R90 cosmids; however, *bus-19(e2966)* mutants were rescued by the R90 cosmid alone. The three new alleles were sequenced and in all cases, changes were identified in the exonic sequence of T07F10.4

(Figure 7). Two alleles, *bus-19(e2964)* and *bus-19(e2965)*, have missense mutations in exon 3 resulting in a G90E and a C102Y amino acid change, respectively. The G90E change in *bus-19(e2964)*, the strongest mutation, affects a highly conserved residue. The *bus-19(e2965)* mutation affects a mildly conserved residue. The weak mutation, *bus-19(e2966)*, has a missense mutation in exon 7, which causes a P235L amino acid change in a less conserved residue. These results indicate that *bus-19* is indeed T07F10.4. The failure of RNAi experiments to phenocopy the Bus phenotype can be ascribed to the low efficiency of RNAi with respect to postembryonic phenotypes, which we have also observed with other *bus* genes. *bus-19(e2964)* was fully rescued with the fosmid clone WRM0640cD03. We achieved partial rescue of *bus-19(e2964)* with both a 7.3- and a 13-kb fragment amplified from fosmid clone WRM0623dE01, which spanned T07F10.4a and T07F10.4a and -b, respectively. This partial rescue corrected the Dpy and Skd phenotypes in both cases; however, the transgenic animals were still Bus on the pathogen. We confirmed the exon/intron boundaries of both T07F10.4a and T07F10.4b by sequencing two cDNA clones, yk1387f02 and yk1345b03, respectively, which were provided by Y. Kohara.

***bus-19* encodes a novel ancient protein:** BUS-19 belongs to the KOG3140/COG0398/DedA predicted membrane protein homology group, members of which exist in all taxa except Archaea and Viruses. No functional information is available for any homolog. The DedA domain occurs in many proteins concurrently with other well-characterized domains, such as a phospholipase D motif and a GlpE rhodanese sulfurtransferase domain. Although DedA-containing proteins are suspected to have transporter function, possibly involved in detoxification processes, the BUS-19/DedA group does not contain any characterized domain (Marchler-Bauer and Bryant 2004; Ledgham *et al.* 2005). ProtFun 2.2 (http://www.cbs.dtu.dk/services/ProtFun/) also predicts a transporter function for BUS-19. Other identifiable protein features of BUS-19 include six transmembrane domains (including a probable signal sequence) and a putative ER localization motif. Other members of KOG3140 include hypothetical proteins in human (Q96HV5), Drosophila (Q9VX39), Saccharomyces (P36164), and two *C. elegans* predicted proteins O62126 (*tag-175*; ORF D2013.10) and Q9XXB4 (ORF Y71A12C.2) (Figure 7). The *C. elegans* homologs of *bus-19*, *tag-175*, and Y71A12C.2 are located on LGII and LGI, respectively. The expression pattern and RNAi effects have been analyzed for *tag-175*; however, these analyses have not led to any further knowledge of its function (Henricson *et al.* 2004). We also examined *tag-175(gk278)*, which is a putative null for this *bus-19* homolog, and observed none of the multiple abnormal phenotypes of *bus-19* mutants, including the Bus phenotype in the presence of *M. nematophilum*, suggesting that *tag-175* is a less important member of this family.

DISCUSSION

Practicality of *Mos1* mutagenesis: Infection of *C. elegans* by the gram-positive bacterium *M. nematophilum* results in a defensive postanal swelling response through activation of an ERK/MAPK signaling pathway (Nicholas and Hodgkin 2004). Over 20 loci are required for infection and/or tail swelling, as revealed in previous EMS and *mut-7* screens, which do not appear to have reached saturation (Gravato-Nobre *et al.* 2005). Three of these genes, *egl-5*, *sur-2*, and *srf-3* were known from earlier unrelated studies, having been characterized for their roles in posterior cell fate, vulval development, and surface properties of the worm, respectively (Chisholm 1991; Link *et al.* 1992; Singh and Han 1995). To quickly identify more genes affecting the *C. elegans/M. nematophilum* interaction, we carried out screens using *Mos1* mutagenesis. *Mos1* insertions in four genes (*egl-8*, *tax-4*, *bus-19*, and *bus-17*) were found to result in a Bus (nonswollen tail) phenotype. Of the 19 *bus* loci identified in previous EMS and *mut-7* mutagenesis screens, an allele of only one locus, *bus-17*, was identified here, which provides further indication that screens for Bus mutants are far from saturated.

Using *Mos1* mutagenesis was therefore an attractive option, due to the large number of genes that can be mutated to resistance to *M. nematophilum* (Gravato-Nobre *et al.* 2005). At the time these screens were carried out, the rate of *Mos1* mutagenesis was estimated to be significantly lower than that of EMS mutagenesis. Confirming this, we recovered Bus mutants at a much lower rate with *Mos1* than with EMS. A clonal screen for EMS Bus mutants formed part of the previous study (Gravato-Nobre *et al.* 2005); this yielded six mutants among 639 F_2 clones, or approximately one mutant for every 30 F_1 animals. The overall efficiency of our *Mos1* screens, yielding a total of four mutants for 7620 F_1 animals, was ~50-fold lower than this. This efficiency is comparable to that reported for a direct comparison of *Mos1* mutagenesis with ENU mutagenesis to identify Osm mutants (Bessereau *et al.* 2001).

Figure 7.—ClustalW (v.1.83) alignment of *bus-19* and homologs. Light gray boxes signify semiconserved substitutions, dark gray boxes signify conserved substitutions, and black boxes signify identical residues. Species are as follows: *Cb*, *Caenorhabditis briggsae*; *Hs*, *Homo sapiens*; *Gg*, *Gallus gallus*; *At*, *Arabidopsis thaliana*; *Dd*, *Dictyostelium discoideum*; *Dm*, *Drosophila melanogaster*; *Gm*, *Geobacter metallireducens*. Bars above the sequence indicate transmembrane domains predicted for BUS-19 by TMHMM2. The amino acid changes caused by EMS in other *bus-19* alleles are noted above the sequence.

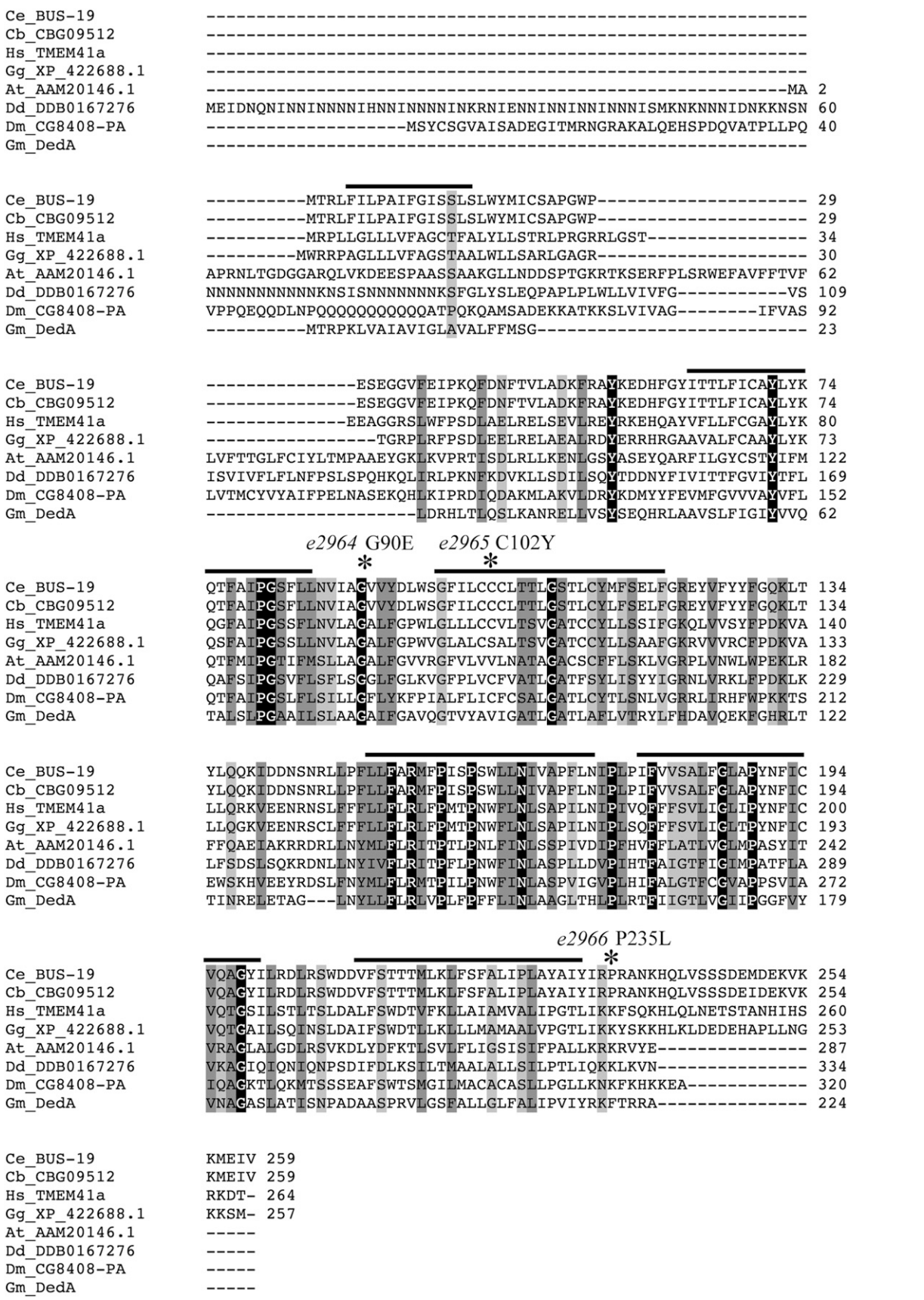
Ce_BUS-19
Cb_CBG09512
Hs_TMEM41a
Gg_XP_422688.1
At_AAM20146.1
Dd_DDB0167276
Dm_CG8408-PA
Gm_DedA
e2964 G90E
e2965 C102Y
e2966 P235L

A previously published pilot experiment using *Mos1* mutagenesis discusses the advantages of using *Mos1* (Granger *et al* 2004). Although we experienced low efficiency and substantial variability in the rate of *Mos1* transposition, these advantages still remain worthwhile. The variability may be due to a number of factors, such as the ancestry and the growth history of the double-array-carrying P_0's, temperature fluctuations during the heat-shock procedure, or time of collection of animals after heat shock (Williams *et al.* 2005). However, since detection of the Bus phenotype is easy, and the number of target genes is quite high, the low efficiency of mutagenesis was offset by the ease and swiftness of identifying the molecular insertions, as demonstrated here by the case of *bus-17*. Further, two mutations, *egl-8* and *bus-19* severely impair the growth of the worm on the pathogen and thus would have been difficult to recover and map in previous screens, but were quickly cloned due to the presence of the *Mos1* molecular tag.

Different stages of the host–pathogen interaction: The genes identified in this and previous studies highlight the different defenses and vulnerabilities of *C. elegans* with respect to *M. nematophilum*. First, *C. elegans* is capable of recognizing and mounting a behavioral avoidance response to the presence of *M. nematophilum* in the environment. We show that this behavioral response involves the action of TAX-4 and TAX-2. *C. elegans* has been shown to mount a behavioral response to other pathogens, which includes learning to avoid them (Pujol *et al.* 2001; Zhang *et al.* 2005). Further, TAX-4 and TAX-2 are involved in the recognition of pathogenic Pseudomonas strains as well, suggesting that they play a general role in pathogen recognition and avoidance. *tax-4* and *tax-2* mutants are defective in many behaviors; in particular, chemosensory and gustatory behaviors are compromised (Dusenbery *et al.* 1975; Bargmann *et al.* 1993; Komatsu *et al.* 1996). However, this role of TAX-4 and TAX-2 in mediating avoidance to *M. nematophilum* does not explain the reduced infection and swelling of *tax-4* and *tax-2* mutants, because these *tax* mutants expose themselves to the contaminated food more than wild-type worms do and would therefore be expected to become sicker than wild-type worms, rather than the reverse. We observed other defects of *tax-4* and *tax-2* mutants, which suggest that these genes can affect the cuticle or surface composition of the worm, as discussed below.

Second, successful infection by *M. nematophilum* must involve elements of the rectal epithelial surface of *C. elegans* that can be recognized and adhered to by the pathogen. Colonization fails to occur in *bus-17* and *bus-19* mutants, suggesting that these surface factors are absent or masked in mutants of this type, perhaps as a result of alterations in cuticle formation. In support of this possibility, we observed cuticle defects in these mutants. The nematode cuticle is a multilayered structure composed of heavily cross-linked collagen and collagen-like molecules, overlaid by an electron-dense epicuticle and topped by a surface coat (glycocalyx) of carbohydrates. The carbohydrates of the surface coat probably provide major targets for pathogens. Cuticle and surface coat composition are molecularly distinct at each developmental stage of the worm (Cox *et al.* 1981). Further, changes in surface coat composition can be induced by environmental factors (Grenache *et al.* 1996).

bus-17 and *bus-19* mutants exhibit cuticle defects similar to other *bus* mutants in the *srf-3* mutant group (Gravato-Nobre *et al.* 2005). In particular, *bus-17* and *bus-19* mutants are Skd, do not allow bacterial adherence by *M. nematophilum*, and bind fluorescently labeled lectins, consistent with alterations in surface coat composition. *srf-3* encodes a nucleotide sugar transporter, the activity of which is required in the synthesis of many glycoconjugates of the worm (Cipollo *et al.* 2004; Hoflich *et al.* 2004). In addition to preventing the adherence of *M. nematophilum* to the rectal epithelium of the worm, mutations in *srf-3* also inhibit the accumulation of Yersinia biofilm (Darby *et al.* 2002; Tan and Darby 2004). Since *M. nematophilum* does not adhere to the head of the worm, it is unlikely that the same receptors are used by both pathogens. Most likely, the different receptors used by the pathogens are subject to the same glycosylation pathways. BUS-17 is predicted to encode a member of the GT31 family. There are 22 predicted *C. elegans* GT31 family members. Other members of this family include BRE-5 and BRE-2, which are required for the post-translational modification of the CRY5B receptor recognized by the *Bacillus thuringiensis* CRY5B toxin. Upon binding to this receptor, Bt toxin forms holes in the intestine of the worm, leading to death (Griffitts *et al.* 2001, 2003). Neither *bre-2* nor *bre-5* mutants appear to affect cuticular properties or susceptibility to *M. nematophilum*. Nevertheless, mutations in these two genes can affect many divergent processes, indicating functions beyond the modification of intestinal glycolipids (Katic *et al.* 2005).

Mutant defects are notably more severe in *bus-19* than in *bus-17*. In addition to the strong lectin staining and Skd phenotypes, *bus-19* mutants exhibit slow growth, dumpiness, and larval lethality and are Daf-d. Because of the pleiotropic nature of the defects of *bus-19* mutants, it is likely that BUS-19 plays a more fundamental role in generating the cuticle of the worm and perhaps is involved in other processes. The biochemical functions of BUS-19 are entirely mysterious at present, despite the existence of related and equally mysterious proteins in many other organisms. It seems likely that these are integral membrane proteins, and the surface alterations we observe suggest that BUS-19 may be involved in trafficking or modification of extracellular molecules, but little more can be said. The *C. elegans bus-19* mutant phenotypes represent the first reports of abnormalities associated with loss of a protein in this family in any organism.

tax-4 mutants also affect colonization by *M. nematophilum*, and the observations of cuticle abnormalities in both *tax-2* and *tax-4* mutants indicate that these genes influence the property of the nematode surface, but their Bus and cuticle phenotypes are variable, in contrast to the fully penetrant effects of strong mutations on *bus-17* and *bus-19*. Moreover, the relevant action of these genes appears to be located in chemosensory neurons, which are unlikely to be directly involved in cuticle synthesis. We propose that TAX-4 and TAX-2 help to coordinate the secretion of components of the cuticle with the proper developmental age of the worm and that in *tax-4* and *tax-2* mutants, the impaired coordination results in abnormal cuticle that is less able to support infection. It is known that TAX-4 and TAX-2 play roles in determining entry and recovery from dauer formation, and changing to and from the dauer state requires alterations in metabolism as well as changes in the structure and composition of the cuticle and surface coat. *tax-4* and *tax-2* mutants exhibit visible and variable abnormalities in their cuticles, which may indicate more subtle defects that influence pathogen adherence. One aspect of the dauer decision that has not been fully explored is the signaling from neuronal to seam cells to coordinate the secretion of cuticle or coat components with the developmental stage of the worm. Changes in surface coat composition can be induced by environmental factors, in part through signaling by *daf-c* genes (Grenache *et al.* 1996). Mutations in *daf-c* genes, including *daf-11*, result in the expression of L1-specific antigens in older-stage animals. Further, it has been noted that surface antigen switching was reduced in *tax-4(p678)* mutants, suggesting a role for TAX-4 in mediating sensory input to cuticle output (Olsen *et al.* 2006).

We did not observe dauer-constitutive *daf-2(e1368)* mutants to have an altered response to *M. nematophilum*, in contrast to the variable Bus phenotype seen for Daf-c *daf-11(m47)* mutants, but the mutant cuticles may well be different in the two cases, such that *daf-2(e1368)* mutants remain fully susceptible to infection. Genes of the DAF-2 insulin/IGF group of the dauer pathway have also been demonstrated to influence the response to lethal pathogens, in part by affecting production of antimicrobial proteins. Specifically, mutations in *daf-2* and *age-1* result in enhanced resistance to killing by *Pseudomonas aeruginosa*, *Enterococcus faecalis*, and *Staphylococcus aureus* (Garsin *et al.* 2003). The DAF-2 insulin-like receptor regulates the expression of antimicrobial effectors, such as *lys-7* and *lys-8* (which encode lysozymes), and the saposin-like gene, *spp-1*, by derepressing the fork-head transcription factor DAF-16 (Murphy *et al.* 2003). In *daf-2* mutants therefore, DAF-16 upregulates the transcription of a number of genes with proposed antimicrobial activities. We did not see any reduced infection or swelling of *daf-2(e1368)* mutants exposed to *M. nematophilum* at room temperature or at 25°. These results suggest that the induced upregulation of DAF-16 antimicrobials in *daf-2* mutants is not protective against *M. nematophilum*. *daf-16(m26)* and *daf-16(mgDf50)* mutants survive well on the pathogen unlike hypersensitive *sur-2* and other ERK/MAP kinase mutants, which suggests that DAF-16 does not play a major protective role against *M. nematophilum* infection. This may not be surprising since *daf-16* mutants were not hypersensitive to killing by lethal pathogens in the study mentioned above (Garsin *et al.* 2003). Moreover, DAF-16 cannot be the only transcription factor contributing to the expression of antimicrobials such as lysozymes, because *lys-7* mutants are severely affected by *M. nematophilum*, surviving exposure to the pathogen much less well than *daf-16* mutants (O'Rourke *et al.* 2006).

Third, *C. elegans* induces a defensive response to the adherence of *M. nematophilum* to rectal epithelia and colonization of the rectum, which includes major swelling of rectal hypodermal cells. Previous work has demonstrated this swelling response to require the action of the members of the ERK/MAP kinase cascade. EGL-8 is most likely to function in this step of the pathogen response. Mutations in *egl-8* result in little or no rectal swelling in infected worms despite bacterial colonization of the rectum. Although EGL-8 is expressed in most of the neurons of the worm, it is also expressed in the posterior intestine (Lackner *et al.* 1999; Miller *et al.* 1999). Recent studies have also indicated that EGL-8 functions in pharyngeal pumping, sperm transfer, and Ca^{2+} oscillation-associated posterior body contractions of the intestine, suggesting that it may function in non-neuronal tissues (Bastiani *et al.* 2003; Steger and Avery 2004; Espelt *et al.* 2005; Gower *et al.* 2005). Whether or not EGL-8 feeds into the ERK/MAP kinase cascade or acts in a parallel pathway remains to be determined. Moreover, *egl-8* mutants are not as hypersensitive to *M. nematophilum* as are ERK/MAP kinase mutants, indicating that the kinase cascade probably contributes to defense in more ways than simply activating rectal swelling.

The analysis of these four mutants reveals the complexity of the interactions between host and pathogen and the multiple contributions of various genes both to immunity and to the normal development and behavior of the worm. If, as seems likely, there has been significant coevolution of *C. elegans* and *M. nematophilum*, such complexity is only to be expected.

We thank the Caenorhabditis Genetics Center for many strains, Ikue Mori for *tax-4* mutants, Cori Bargmann for *tax-2* mutants, Mario de Bono for the rescuing *tax-4::*GFP and *odr-4p::tax-4::*GFP constructs, Yuji Kohara for cDNA clones, Don Moerman and Jaryn Perkins for fosmid clones, Gail Preston for Pseudomonas strains, members of the André Furger lab for help with the *bus-17* molecular characterization, and anonymous reviewers for constructive criticisms. Jean-Louis Bessereau provided essential guidance with *Mos1* mutagenesis, Creg Darby generously shared unpublished results on Yersinia, and Chris Ponting supplied useful thoughts on BUS-19. Members of the Hodgkin and Darby labs provided invaluable expertise and discussion. K.Y. was supported in part by a Ruth L. Kirschstein National Research Service Award from the National Institutes of Health. This work was supported by the Medical Research Council (United Kingdom).

LITERATURE CITED

Baba, T., T. Shimizu, Y. Suzuki, M. Ogawara, K. Isono *et al.*, 2005 Estrogen, insulin, and dietary signals cooperatively regulate longevity signals to enhance resistance to oxidative stress in mice. J. Biol. Chem. **280:** 16417–16426.

Bargmann, C. I., and H. R. Horvitz, 1991a Chemosensory neurons with overlapping functions direct chemotaxis to multiple chemicals in *C. elegans*. Neuron **7:** 729–742.

Bargmann, C. I., and H. R. Horvitz, 1991b Control of larval development by chemosensory neurons in *Caenorhabditis elegans*. Science **251:** 1243–1246.

Bargmann, C. I., E. Hartwieg and H. R. Horvitz, 1993 Odorant-selective genes and neurons mediate olfaction in *C. elegans*. Cell **74:** 515–527.

Bastiani, C. A., S. Gharib, M. I. Simon and P. W. Sternberg, 2003 *Caenorhabditis elegans* Galphaq regulates egg-laying behavior via a PLCbeta-independent and serotonin-dependent signaling pathway and likely functions both in the nervous system and in muscle. Genetics **165:** 1805–1822.

Bessereau, J. L., A. Wright, D. C. Williams, K. Schuske, M. W. Davis *et al.*, 2001 Mobilization of a Drosophila transposon in the *Caenorhabditis elegans* germ line. Nature **413:** 70–74.

Birnby, D. A., E. M. Link, J. J. Vowels, H. Tian, P. L. Colacurcio *et al.*, 2000 A transmembrane guanylyl cyclase (DAF-11) and Hsp90 (DAF-21) regulate a common set of chemosensory behaviors in *Caenorhabditis elegans*. Genetics **155:** 85–104.

Blaxter, M. L., and D. Bird, 1997 Parasitic nematodes, pp. 851–878 in *C. elegans II*, edited by D. L. Riddle, T. Blumenthal, B. J. Meyer and J. R. Priess. Cold Spring Harbor Laboratory Press, Plainview, NY.

Brenner, S., 1974 The genetics of *Caenorhabditis elegans*. Genetics **77:** 71–94.

Chisholm, A., 1991 Control of cell fate in the tail region of *C. elegans* by the gene *egl-5*. Development **111:** 921–932.

Cipollo, J. F., A. M. Awad, C. E. Costello and C. B. Hirschberg, 2004 *srf-3*, a mutant of *Caenorhabditis elegans*, resistant to bacterial infection and to biofilm binding, is deficient in glycoconjugates. J. Biol. Chem. **279:** 52893–52903.

Coburn, C. M., and C. I. Bargmann, 1996 A putative cyclic nucleotide-gated channel is required for sensory development and function in *C. elegans*. Neuron **17:** 695–706.

Cox, G. N., S. Staprans and R. S. Edgar, 1981 The cuticle of *Caenorhabditis elegans*. II. Stage-specific changes in ultrastructure and protein composition during postembryonic development. Dev. Biol. **86:** 456–470.

Darby, C., J. W. Hsu, N. Ghori and S. Falkow, 2002 *Caenorhabditis elegans*: plague bacteria biofilm blocks food intake. Nature **417:** 243–244.

de Bono, M., D. M. Tobin, M. W. Davis, L. Avery and C. I. Bargmann, 2002 Social feeding in *Caenorhabditis elegans* is induced by neurons that detect aversive stimuli. Nature **419:** 899–903.

Dusenbery, D. B., R. E. Sheridan and R. L. Russell, 1975 Chemotaxis-defective mutants of the nematode *Caenorhabditis elegans*. Genetics **80:** 297–309.

Espelt, M. V., A. Y. Estevez, X. Yin and K. Strange, 2005 Oscillatory Ca2+ signaling in the isolated *Caenorhabditis elegans* intestine: role of the inositol-1,4,5-trisphosphate receptor and phospholipases C beta and gamma. J. Gen. Physiol. **126:** 379–392.

Gami, M. S., and C. A. Wolkow, 2006 Studies of *Caenorhabditis elegans* DAF-2/insulin signaling reveal targets for pharmacological manipulation of lifespan. Aging Cell **5:** 31–37.

Garsin, D. A., J. M. Villanueva, J. Begun, D. H. Kim, C. D. Sifri *et al.*, 2003 Long-lived *C. elegans daf-2* mutants are resistant to bacterial pathogens. Science **300:** 1921.

Gems, D., A. J. Sutton, M. L. Sundermeyer, P. S. Albert, K. V. King *et al.*, 1998 Two pleiotropic classes of *daf-2* mutation affect larval arrest, adult behavior, reproduction and longevity in *Caenorhabditis elegans*. Genetics **150:** 129–155.

Gower, N. J., D. S. Walker and H. A. Baylis, 2005 Inositol 1,4,5-trisphosphate signaling regulates mating behavior in *Caenorhabditis elegans* males. Mol. Biol. Cell **16:** 3978–3986.

Granger, L., E. Martin and L. Segalat, 2004 *Mos* as a tool for genome-wide insertional mutagenesis in *Caenorhabditis elegans*: results of a pilot study. Nucleic Acids Res. **32:** e117.

Gravato-Nobre, M. J., and J. Hodgkin, 2005 *Caenorhabditis elegans* as a model for innate immunity to pathogens. Cell Microbiol. **7:** 741–751.

Gravato-Nobre, M. J., H. R. Nicholas, R. Nijland, D. O'Rourke, D. E. Whittington *et al.*, 2005 Multiple genes affect sensitivity of *Caenorhabditis elegans* to the bacterial pathogen *Microbacterium nematophilum*. Genetics **171:** 1033–1045.

Grenache, D. G., I. Caldicott, P. S. Albert, D. L. Riddle and S. M. Politz, 1996 Environmental induction and genetic control of surface antigen switching in the nematode *Caenorhabditis elegans*. Proc. Natl. Acad. Sci. USA **93:** 12388–12393.

Griffitts, J. S., J. L. Whitacre, D. E. Stevens and R. V. Aroian, 2001 Bt toxin resistance from loss of a putative carbohydrate-modifying enzyme. Science **293:** 860–864.

Griffitts, J. S., D. L. Huffman, J. L. Whitacre, B. D. Barrows, L. D. Marroquin *et al.*, 2003 Resistance to a bacterial toxin is mediated by removal of a conserved glycosylation pathway required for toxin-host interactions. J. Biol. Chem. **278:** 45594–45602.

Hedgecock, E. M., and R. L. Russell, 1975 Normal and mutant thermotaxis in the nematode *Caenorhabditis elegans*. Proc. Natl. Acad. Sci. USA **72:** 4061–4065.

Henricson, A., E. L. Sonnhammer, D. L. Baillie and A. V. Gomes, 2004 Functional characterization in *Caenorhabditis elegans* of transmembrane worm-human orthologs. BMC Genomics **5:** 85.

Hodgkin, J., P. E. Kuwabara and B. Corneliussen, 2000 A novel bacterial pathogen, *Microbacterium nematophilum*, induces morphological change in the nematode *C. elegans*. Curr. Biol. **10:** 1615–1618.

Hoflich, J., P. Berninsone, C. Gobel, M. J. Gravato-Nobre, B. J. Libby *et al.*, 2004 Loss of *srf-3*-encoded nucleotide sugar transporter activity in *Caenorhabditis elegans* alters surface antigenicity and prevents bacterial adherence. J. Biol. Chem. **279:** 30440–30448.

James, S. R., and C. P. Downes, 1997 Structural and mechanistic features of phospholipases C: effectors of inositol phospholipid-mediated signal transduction. Cell Signal **9:** 329–336.

Jannson, H. B., 1994 Adhesion of conidia of *Drechmeria coniospora* to *Caenorhabditis elegans* wild type and mutants. J. Nematol. **26:** 430–435.

Johnson, K. F., 1999 Synthesis of oligosaccharides by bacterial enzymes. Glycoconj. J. **16:** 141–146.

Joshua, G. W., A. V. Karlyshev, M. P. Smith, K. E. Isherwood, R. W. Titball *et al.*, 2003 A *Caenorhabditis elegans* model of Yersinia infection: biofilm formation on a biotic surface. Microbiology **149:** 3221–3229.

Katic, I., L. G. Vallier and I. Greenwald, 2005 New positive regulators of *lin-12* activity in *Caenorhabditis elegans* include the BRE-5/Brainiac glycosphingolipid biosynthesis enzyme. Genetics **171:** 1605–1615.

Kenyon, C., J. Chang, E. Gensch, A. Rudner and R. Tabtiang, 1993 A *C. elegans* mutant that lives twice as long as wild type. Nature **366:** 461–464.

Komatsu, H., I. Mori, J. S. Rhee, N. Akaike and Y. Ohshima, 1996 Mutations in a cyclic nucleotide-gated channel lead to abnormal thermosensation and chemosensation in *C. elegans*. Neuron **17:** 707–718.

Komatsu, H., Y. H. Jin, N. L'Etoile, I. Mori, C. I. Bargmann *et al.*, 1999 Functional reconstitution of a heteromeric cyclic nucleotide-gated channel of *Caenorhabditis elegans* in cultured cells. Brain Res. **821:** 160–168.

Korf, I., P. Flicek, D. Duan and M. R. Brent, 2001 Integrating genomic homology into gene structure prediction. Bioinformatics **17**(Suppl. 1): S140–S148.

Lackner, M. R., S. J. Nurrish and J. M. Kaplan, 1999 Facilitation of synaptic transmission by EGL-30 Gqalpha and EGL-8 PLCbeta: DAG binding to UNC-13 is required to stimulate acetylcholine release. Neuron **24:** 335–346.

Ledgham, F., B. Quest, T. Vallaeys, M. Mergeay and J. Coves, 2005 A probable link between the DedA protein and resistance to selenite. Res. Microbiol. **156:** 367–374.

Link, C. D., M. A. Silverman, M. Breen, K. E. Watt and S. A. Dames, 1992 Characterization of *Caenorhabditis elegans* lectin-binding mutants. Genetics **131:** 867–881.

Marchler-Bauer, A., and S. H. Bryant, 2004 CD-Search: protein domain annotations on the fly. Nucleic Acids Res. **32:** W327–W331.

Mello, C. C., J. M. Kramer, D. Stinchcomb and V. Ambros, 1991 Efficient gene transfer in *C. elegans*: extrachromosomal maintenance and integration of transforming sequences. EMBO J. **10:** 3959–3970.

Mendoza de Gives, P., K. G. Davies, M. Morgan and J. M. Behnke, 1999 Attachment tests of Pasteuria penetrans to the cuticle of plant and animal parasitic nematodes, free living nematodes and srf mutants of *Caenorhabditis elegans*. J. Helminthol. **73:** 67–71.

Miller, K. G., M. D. Emerson and J. B. Rand, 1999 Goalpha and diacylglycerol kinase negatively regulate the Gqalpha pathway in *C. elegans*. Neuron **24:** 323–333.

Millet, A. C., and J. J. Ewbank, 2004 Immunity in *Caenorhabditis elegans*. Curr. Opin. Immunol. **16:** 4–9.

Murphy, C. T., S. A. McCarroll, C. I. Bargmann, A. Fraser, R. S. Kamath *et al.*, 2003 Genes that act downstream of DAF-16 to influence the lifespan of *Caenorhabditis elegans*. Nature **424:** 277–283.

Nicholas, H. R., and J. Hodgkin, 2004 The ERK MAP kinase cascade mediates tail swelling and a protective response to rectal infection in *C. elegans*. Curr. Biol. **14:** 1256–1261.

Olsen, D. P., D. Phu, L. J. Libby, J. A. Cormier, K. M. Montez *et al.*, 2006 Chemosensory control of surface antigen switching in the nematode *Caenorhabditis elegans*. Genes Brain Behav. (in press).

O'Rourke, D., D. Baban, M. Demidova, R. Mott and J. Hodgkin, 2006 Genomic clusters, putative pathogen recognition molecules and antimicrobial genes are induced by infection of *C. elegans* with *M. nematophilum*. Genome Res. **16:** 1005–1016.

Pujol, N., E. M. Link, L. X. Liu, C. L. Kurz, G. Alloing *et al.*, 2001 A reverse genetic analysis of components of the Toll signaling pathway in *Caenorhabditis elegans*. Curr. Biol. **11:** 809–821.

Satterlee, J. S., W. S. Ryu and P. Sengupta, 2004 The CMK-1 CaMKI and the TAX-4 cyclic nucleotide-gated channel regulate thermosensory neuron gene expression and function in *C. elegans*. Curr. Biol. **14:** 62–68.

Schulenburg, H., C. L. Kurz and J. J. Ewbank, 2004 Evolution of the innate immune system: the worm perspective. Immunol. Rev. **198:** 36–58.

Sifri, C. D., J. Begun and F. M. Ausubel, 2005 The worm has turned—microbial virulence modeled in *Caenorhabditis elegans*. Trends Microbiol. **13:** 119–127.

Singh, N., and M. Han, 1995 *sur-2*, a novel gene, functions late in the *let-60* ras-mediated signaling pathway during *Caenorhabditis elegans* vulval induction. Genes Dev. **9:** 2251–2265.

Steger, K. A., and L. Avery, 2004 The GAR-3 muscarinic receptor cooperates with calcium signals to regulate muscle contraction in the *Caenorhabditis elegans* pharynx. Genetics **167:** 633–643.

Tan, L., and C. Darby, 2004 A movable surface: formation of Yersinia sp. biofilms on motile *Caenorhabditis elegans*. J. Bacteriol. **186:** 5087–5092.

Tatar, M., A. Bartke and A. Antebi, 2003 The endocrine regulation of aging by insulin-like signals. Science **299:** 1346–1351.

Thomas, J. H., D. A. Birnby and J. J. Vowels, 1993 Evidence for parallel processing of sensory information controlling dauer formation in *Caenorhabditis elegans*. Genetics **134:** 1105–1117.

Wicks, S. R., C. J. de Vries, H. G. van Luenen and R. H. Plasterk, 2000 CHE-3, a cytosolic dynein heavy chain, is required for sensory cilia structure and function in *Caenorhabditis elegans*. Dev. Biol. **221:** 295–307.

Wicks, S. R., R. T. Yeh, W. R. Gish, R. H. Waterston and R. H. Plasterk, 2001 Rapid gene mapping in *Caenorhabditis elegans* using a high density polymorphism map. Nat. Genet. **28:** 160–164.

Williams, D. C., T. Boulin, A. F. Ruaud, E. M. Jorgensen and J. L. Bessereau, 2005 Characterization of *Mos1*-mediated mutagenesis in *Caenorhabditis elegans*: a method for the rapid identification of mutated genes. Genetics **169:** 1779–1785.

Yochem, J., T. Gu and M. Han, 1998 A new marker for mosaic analysis in *Caenorhabditis elegans* indicates a fusion between hyp6 and hyp7, two major components of the hypodermis. Genetics **149:** 1323–1334.

Zhang, Y., H. Lu and C. I. Bargmann, 2005 Pathogenic bacteria induce aversive olfactory learning in *Caenorhabditis elegans*. Nature **438:** 179–184.

Communicating editor: A. Villeneuve